(12) INTERNATIONAL APPLICATION PUBLISHED UNDER THE PATENT COOPERATION TREATY (PCT)

(19) World Intellectual Property Organization
International Bureau

(43) International Publication Date
27 September 2012 (27.09.2012)

WIPO | PCT

(10) International Publication Number
WO 2012/126070 A1

(51) International Patent Classification:
G06T 7/00 (2006.01)

(21) International Application Number:
PCT/BE2012/000017

(22) International Filing Date:
26 March 2012 (26.03.2012)

(25) Filing Language: English

(26) Publication Language: English

(30) Priority Data:
US61/465,875 24 March 2011 (24.03.2011) US

(71) Applicant *(for all designated States except US)*: **KATHOLIEKE UNIVERSITEIT LEUVEN** [BE/BE]; K.U. Leuven R&D, Waaistraat 6- bus 5105, B-3000 Leuven (BE).

(72) Inventors; and

(75) Inventors/Applicants *(for US only)*: **ADRIAENSSENS, Tom** [BE/BE]; Boetsenberg 3, B-3053 Haasrode (BE). **UGHI, Giovanni, Jacopo** [IT/BE]; Tervursestraat 117, Bus 11, B-3000 Leuven (BE). **DESMET, Walter** [BE/BE]; Arnoudt Rulenslaan 28, B-3020 Herent (BE). **DHOOGE, Jan** [BE/BE]; Leegheid 9, B-2800 Mechelen (BE).

(74) Common Representative: **KATHOLIEKE UNIVERSITEIT LEUVEN**; K.U. Leuven R&D, Waaistraat 6-bus 5105, B-3000 Leuven (BE).

(81) Designated States *(unless otherwise indicated, for every kind of national protection available)*: AE, AG, AL, AM, AO, AT, AU, AZ, BA, BB, BG, BH, BR, BW, BY, BZ, CA, CH, CL, CN, CO, CR, CU, CZ, DE, DK, DM, DO, DZ, EC, EE, EG, ES, FI, GB, GD, GE, GH, GM, GT, HN, HR, HU, ID, IL, IN, IS, JP, KE, KG, KM, KN, KP, KR, KZ, LA, LC, LK, LR, LS, LT, LU, LY, MA, MD, ME, MG, MK, MN, MW, MX, MY, MZ, NA, NG, NI, NO, NZ, OM, PE, PG, PH, PL, PT, QA, RO, RS, RU, RW, SC, SD, SE, SG, SK, SL, SM, ST, SV, SY, TH, TJ, TM, TN, TR, TT, TZ, UA, UG, US, UZ, VC, VN, ZA, ZM, ZW.

(84) Designated States *(unless otherwise indicated, for every kind of regional protection available)*: ARIPO (BW, GH, GM, KE, LR, LS, MW, MZ, NA, RW, SD, SL, SZ, TZ, UG, ZM, ZW), Eurasian (AM, AZ, BY, KG, KZ, MD, RU, TJ, TM), European (AL, AT, BE, BG, CH, CY, CZ, DE, DK, EE, ES, FI, FR, GB, GR, HR, HU, IE, IS, IT, LT, LU, LV, MC, MK, MT, NL, NO, PL, PT, RO, RS, SE, SI, SK, SM, TR), OAPI (BF, BJ, CF, CG, CI, CM, GA, GN, GQ, GW, ML, MR, NE, SN, TD, TG).

[Continued on next page]

(54) Title: AUTOMATIC VOLUMETRIC ANALYSIS AND 3D REGISTRATION OF CROSS SECTIONAL OCT IMAGES OF A STENT IN A BODY VESSEL

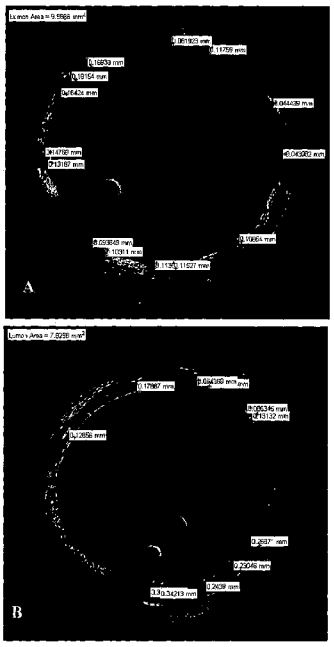

Figure 1

(57) Abstract: A computer based method of automated volumetric stent analysis and OCT pullbacks (datasets) registration in time comprising computer based analysing of multiple images from in- vivo acquired cross sectional OCT images, recorded by an OCT catheter pullback at baseline (freshly implanted device) and at any time point thereafter, of long vessel segments of stent formed by strut from bars in a body vessel (e.g. vascular) the method comprising automatic distance identification and measurement of the separate surfaces zones of said implant device to vessel wall (apposition) and/or covering neointima (corresponding to vessel healing after implantation of the implant device) and the method being characterised in that 1) individual stent struts coverage and apposition and further areas and volumes of separate surfaces zones of a) said implant device to vessel wall (apposition) or b) of neointima coverage are volumetric measured by clustering of neointima coverage according to their spatial 3D location through analysis of equally spaced consecutive OCT cross sectional images or by automatically clustering uncovered (malapposition) struts according to their 3D spatial position through consecutive cross sectional images and 2) registration of intravascular OCT pullbacks recordings (IV-OCT datasets) of points of long vessel segments of transluminal implant device but at different time points of the implantation period comprising a) 3D alignment by rotation and translation and b) refinement of the registration by a registration algorithm (e.g. Interactive closest point (ICP)) and iteratively at a multi-resolution.

WO 2012/126070 A1

Declarations under Rule 4.17:

— *of inventorship (Rule 4.17(iv))*

Published:

— *with international search report (Art. 21(3))*

— *before the expiration of the time limit for amending the claims and to be republished in the event of receipt of amendments (Rule 48.2(h))*

AUTOMATIC VOLUMETRIC ANALYSIS AND 3D REGISTRATION OF CROSS SECTIONAL OCT IMAGES OF A STENT IN A BODY VESSEL

Background and Summary

BACKGROUND OF THE INVENTION

A. Field of the Invention

The present invention relates generally to diagnosing late incomplete stent apposition and coverage via optical coherence tomography at multiple time points and, more particularly to a system and method for diagnosing late incomplete stent apposition and lack of coverage and comparing same vessel slice on an image level or for diagnosing the severity of stent malapposition and uncoverage by computer automated volumetric analysis and three dimensional (3D) registration of optical coherence images of a stent in body vessel.

Several documents are cited throughout the text of this specification. Each of the documents herein (including any manufacturer's specifications, instructions etc.) are hereby incorporated by reference; however, there is no admission that any document cited is indeed prior art of the present invention.

B. Description of the Related Art

ISA (incomplete stent apposition) or stent malapposition is defined as the absence of contact between stent struts and the vessel wall not overlying a side branch. Stent coverage is defined as the presence of a thin layer of neointimal tissue covering metallic stent surface. Given the relatively small dimensions of intracoronary stent struts and the relatively poor spatial resolution of non-invasive imaging techniques and even coronary angiography, they can only be detected and quantified by means of intracoronary imaging; intravascular ultrasound (IVUS) and –more recently-optical coherence tomography (OCT), the latter having a resolution of 10-15 μm (10 times better than IVUS). Acute ISA (detected immediately after stent implantation) is differentiated from late ISA (LAISA). No adverse events appear to be associated with acute ISA. Patients with LAISA have no ISA at the time of stent implantation, but ISA

is detected at follow-up. Its degree can vary from one malapposed strut to true coronary aneurysm formation. IVUS studies have shown that LAISA is more frequent after DES (10%-20%) than BMS (5%-10%) implantation. Compared with these IVUS studies, recent studies with OCT point to a higher incidence of LAISA, especially in patients with acute coronary syndromes. Lack of coverage has been associated with thrombus formation and more in general to BMS and DES failure.

Conflicting data exist concerning the clinical importance (predominantly the association with stent thrombosis) of LAISA. It is plausible that modest ISA is less likely to be clinically relevant as opposed to more severe ISA, which seems to be more likely to result in clinical sequelae. Moreover LAISA has been associated to lack of coverage.

We previously developed an automated algorithm for detection and quantification of malapposition and lack of coverage of intracoronary stent struts (WO2011135103)

Reflecting the greater importance of severe malapposition and lack of coverage with multiple adjacent struts involved as compared to isolated malapposition, by present invention is now provided a software tool to categorize malapposition into clusters (defined as several adjacent malapposed struts) and quantify the severity of malapposition/lack of coverage in these clusters according to several parameters (number of malapposed/ucovered struts, malapposition area and neointimal tissue (coverage) area, volume of malapposition and neointimal tissue (coverage volume)). Stent struts apposition and coverage is additionally monitored and analysis at different time points after stent implantation (months and years).

SUMMARY OF THE INVENTION

In accordance with the purpose of the invention, as embodied and broadly described herein, the invention is broadly drawn to a method of automatic image analysis to an accurately diagnose late incomplete stent apposition and coverage and registering OCT datasets of a same vessel and device through time.

One aspect of the invention concerns a computer based method of automated volumetric stent analysis comprising computer based analysing of multiple images from in-vivo acquired cross sectional OCT images, recorded by an OCT catheter pullback at baseline (freshly implanted device) and at any time point thereafter, of long vessel segments of stent formed by strut from bars in a body vessel (e.g. vascular) the method comprising automatic distance identification and measurement of the separate surfaces zones of said implant device to vessel wall (apposition) and/or covering neointima (corresponding to vessel healing after implantation of the implant device) and the method being **characterised in that** 1) further areas and volumes of separate surfaces zones of a) said implant device to vessel wall (apposition) or b) of neointima coverage are volumetric measured by clustering of neointima coverage according to their spatial 3D location through analysis of equally spaced consecutive OCT cross sectional images or by automatically clustering uncovered (malapposition) struts according to their 3D spatial position through consecutive cross sectional images and 2) registration of two clouds from pullback recordings of points of long vessel segments of transluminal implant device but at different time points of the implantation period comprising a) 3D alignment by rotation and b) refinement of the registration by a closes point registration algorithm (e.g. Interactive closest point (ICP)). This system allows analysing malapposition as a volume and not only as every strut individually (clustering of malapposed struts according to their spatial 3D location to measure). Hereby the malapposed/uncovered struts can be divided into different groups and for every group relevant properties are quantified. In a particular embodiment for each frame the proposed method concerns completely automatic detection (segmentation) of stent struts and lumen and consecutively, discrimination of apposed from malapposed struts is obtained with the use of a threshold computed as A_T (apposition threshold) = strut thickness + polymer thickness (in case of drug eluting stents) + blooming artefacts whereby if strut individual apposition > A_T the strut is labelled as malapposed, otherwise opposed such that 3D position of every strut and discrimination between apposed and clustered malapposed struts is obtained. These malapposed (uncovered) struts can be into different groups according to their 3D position in space and consequently for every cluster, properties like relative long-axis position, length in long-axis direction, angle distribution, number of struts belonging to the group and maximum, minimum and mean strut malapposition values is

quantified. Hereby of a stented sector the number and percentage of apposed and malapposed (covered uncovered) struts, the number of embedded and protruding struts and/or the number of isolated malapposed struts and clusters can be measured. In these methods as a first end-point, for every located cluster, the volume of the whole malapposition (i.e. space between stent to vessel wall) is preferably quantified by 1) stent shape delineation and 2) scan conversion to pixels followed by image quantification involving a) strut by strut individual apposition and/or neointima coverage analysis and b) lumen area and/or stent area analysis and 3) computing the relative difference between lumen area and stent area and 3) volumetric quantification of the apposition area and/or neointimal tissue area through consecutive cross sectional images for volume estimation lumen volume, stent volume and the apposition volume or neointimal tissue volume. The used algorithmic clustering technique is adapted to define groups of variables with homogenous properties within the group they belong to and inhomogeneous properties between other groups. Such algorithmic clustering technique is preferably a non-supervised clustering techniques based on distance measurements (in order to cluster malapposed struts) whereby clusters are defined through a hierarchical agglomerative clustering algorithm composed of three steps (1) definition of a distance measure (for example Euclidean distance), (2) computation of the pair-wise distance matrix D between all the elements and (3) iterative fusion of the 2 most similar elements in a cluster and updating of matrix D (e.g. Single Linkage (SL)). Such algorithm produces as output a *hierarchical tree* which starts from *leaves* (single strut) and ends into a super-cluster containing all the struts of an analysed long vessel zone of a stent in a body vessel. This *hierarchical tree* is obtained through subsequent fusion of elements in clusters becoming bigger step by step (agglomerative methods) and whereby the number of the clusters is dependent on the level at which the tree is observed.

In the clustering step of these above described embodiments the final choose of the number of clusters can be carried out manually (pre-setting at which level the tree is observed) by the user. Hereby the final choose of the number of clusters can be through a cut-off value.

In these embodiments described here above in the stent strut coordinates of two pullbacks of the same stented vessel at different times 1) the position of stent struts

in 3D space and 2) a reconstruction of the stent structure as clouds of points is computed and starting from these data match the two clouds by an algorithm for registration of clouds of points (for example ICP, iterative closest points).Hereby OCT alignment of a dataset of two pullbacks of the same stented vessel at different times can comprise a first step of computing 3D structures aligned according to same centre and same long-axis direction. For examples such the centre of mass of both OCT pullbacks can be computed using the strut coordinates as a system of particles according to the following function:

$$C_M = \frac{\sum_{i=1}^{N} m_i r_i}{\sum_{i=1}^{N} m_i}$$

setting the mass of all the strut particles equals to 1. The 3D datasets can hereby consequently be shifted through the 3D space in order to match the two centres of mass and the moments of inertia of the two objects are then computed and the 3D datasets consecutively aligned in the long-axis direction (z) and the moment of inertia of a rigid object of N point masses m_i can be computed as in the following matrix:

$$I = \begin{matrix} I_{11} & I_{12} & I_{13} \\ I_{21} & I_{22} & I_{23} \\ I_{31} & I_{32} & I_{33} \end{matrix}$$

with:

$$I_{11} = \sum_{i=1}^{N} m_i (y_k^2 + z_k^2) \quad I_{22} = \sum_{i=1}^{N} m_i (x_k^2 + z_k^2) \quad I_{33} = \sum_{i=1}^{N} m_i (x_k^2 + y_k^2)$$

$$I_{12} = -\sum_{i=1}^{N} m_i x_k y_k \quad I_{13} = -\sum_{i=1}^{N} m_i x_k z_k \quad I_{23} = -\sum_{i=1}^{N} m_i y_k z_k$$

and hereby the two datasets through the Eigen vectors of matrix I can be aligned in the long axis direction.

This can by further embodied in that after matching the centres of mass and aligning the two datasets in the long-axis direction; correct 3D rotation is estimated through the use of cost function. Such cost function can be defined between two surfaces S_1 and S_2 as follows:

$$f_{cost}(S_1,S_2)=\frac{1}{N}\sum_{i=1}^{N}(f_{dist}(p_i,S_1))^2 \quad \forall p_i \in S_2$$

with N the number of points belonging to S_2 whereby p_i represent a point in the Euclidean space and S a surface in the same space, the distance between p_i and S is defined as:

$$f_{dist}(p_i,S)=\min(\|p_i-p_s\|^2) \quad \forall p_s \in S$$

and whereby iteratively rotating S_2 of a predefined small angle α (i.e. 2°) from 0° to 360° and computing $f_{cost}(S_1,S_2)$ at every step, the cost function gives information about the distance between the two objects for every possible rotation (figure 11) and whereby minimization of the cost function f_{cost} will result in the rotation able to match the two 3D objects. After minimization of the cost functions, registration between the two clouds of points is refinable through algorithms for difference minimization. A suitable method for finally matching the two clouds is through ICP (iterative closest points). Hereby an output of translation matrix and rotation matrix (rototranslation matrix) is provided.

Yet another embodiment of present invention is use of the method according to embodiments of present invention (here above described) to compare 3D intravascular OCT datasets frame-to-frame. This can be used on pullbacks of the same vessel at different intervals (e.g. baseline, 3 months, 6 months and 9 months) to measure or follow the vessel healing process, after stent implantation, comparing corresponding frames at the different time intervals (e.g. baseline, 3 months, 6 months and 9 months; to assessment on how human coronary arteries react at implantation of different kinds of stents or to asses on how human coronary arteries react after stent implantation on drug treatments.

Yet another embodiment of present invention is an OCT apparatus with a processor adapted to receive input signals generated by pullbacks of an OCT catheter whereby the processer comprises an algorithm to carry out data processing according to any one of methods described here above. .

Further scope of applicability of the present invention will become apparent from the detailed description given hereinafter. However, it should be understood that the

detailed description and specific examples, while indicating preferred embodiments of the invention, are given by way of illustration only, since various changes and modifications within the spirit and scope of the invention will become apparent to those skilled in the art from this detailed description. It is to be understood that both the foregoing general description and the following detailed description are exemplary and explanatory only and are not restrictive of the invention, as claimed.

Detailed Description

DETAILED DESCRIPTION OF EMBODIMENTS OF THE INVENTION

The following detailed description of the invention refers to the accompanying drawings. The same reference numbers in different drawings identify the same or similar elements. Also, the following detailed description does not limit the invention. Instead, the scope of the invention is defined by the appended claims and equivalents thereof.

The following detailed description of the invention refers to the accompanying drawings. The same reference numbers in different drawings identify the same or similar elements. Also, the following detailed description does not limit the invention. Instead, the scope of the invention is defined by the appended claims and equivalents thereof.

Several documents are cited throughout the text of this specification. Each of the documents herein (including any manufacturer's specifications, instructions etc.) are hereby incorporated by reference; however, there is no admission that any document cited is indeed prior art of the present invention.

The present invention will be described with respect to particular embodiments and with reference to certain drawings but the invention is not limited thereto but only by the claims. The drawings described are only schematic and are non-limiting. In the drawings, the size of some of the elements may be exaggerated and not drawn to

scale for illustrative purposes. The dimensions and the relative dimensions do not correspond to actual reductions to practice of the invention.

Furthermore, the terms first, second, third and the like in the description and in the claims, are used for distinguishing between similar elements and not necessarily for describing a sequential or chronological order. It is to be understood that the terms so used are interchangeable under appropriate circumstances and that the embodiments of the invention described herein are capable of operation in other sequences than described or illustrated herein.

Moreover, the terms top, bottom, over, under and the like in the description and the claims are used for descriptive purposes and not necessarily for describing relative positions. It is to be understood that the terms so used are interchangeable under appropriate circumstances and that the embodiments of the invention described herein are capable of operation in other orientations than described or illustrated herein.

It is to be noticed that the term "comprising", used in the claims, should not be interpreted as being restricted to the means listed thereafter; it does not exclude other elements or steps. It is thus to be interpreted as specifying the presence of the stated features, integers, steps or components as referred to, but does not preclude the presence or addition of one or more other features, integers, steps or components, or groups thereof. Thus, the scope of the expression "a device comprising means A and B" should not be limited to the devices consisting only of components A and B. It means that with respect to the present invention, the only relevant components of the device are A and B.

Reference throughout this specification to "one embodiment" or "an embodiment" means that a particular feature, structure or characteristic described in connection with the embodiment is included in at least one embodiment of the present invention. Thus, appearances of the phrases "in one embodiment" or "in an embodiment" in various places throughout this specification are not necessarily all referring to the same embodiment, but may. Furthermore, the particular features, structures or

characteristics may be combined in any suitable manner, as would be apparent to one of ordinary skill in the art from this disclosure, in one or more embodiments.

Similarly it should be appreciated that in the description of exemplary embodiments of the invention, various features of the invention are sometimes grouped together in a single embodiment, figure, or description thereof for the purpose of streamlining the disclosure and aiding the understanding of one or more of the various inventive aspects. This method of disclosure, however, is not to be interpreted as reflecting an intention that the claimed invention requires more features than are expressly recited in each claim. Rather, as the following claims reflect, inventive aspects lie in less than all features of a single foregoing disclosed embodiment. Thus, the claims following the detailed description are hereby expressly incorporated into this detailed description, with each claim standing on its own as a separate embodiment of this invention.

Furthermore, while some embodiments described herein include some but not other features included in other embodiments, combinations of features of different embodiments are meant to be within the scope of the invention, and form different embodiments, as would be understood by those in the art. For example, in the following claims, any of the claimed embodiments can be used in any combination.

In the description provided herein, numerous specific details are set forth. However, it is understood that embodiments of the invention may be practiced without these specific details. In other instances, well-known methods, structures and techniques have not been shown in detail in order not to obscure an understanding of this description.

Other embodiments of the invention will be apparent to those skilled in the art from consideration of the specification and practice of the invention disclosed herein.
It is intended that the specification and examples be considered as exemplary only.
Each and every claim is incorporated into the specification as an embodiment of the present invention. Thus, the claims are part of the description and are a further description and are in addition to the preferred embodiments of the present invention.
Each of the claims set out a particular embodiment of the invention.
The following terms are provided solely to aid in the understanding of the invention.

Definitions

A stent is a transluminal implant device or a longitudinal tubular implant device formed by strut from bars. It is a vascular stent when the transluminal implant device is for vascular vessels.

Stent malapposition is defined as the absence of contact between stent struts and the vessel wall not overlying a side branch

An automated algorithm for detection and quantification of malapposition of intracoronary stent struts.

A computer based method was developed in our group for analysing the behaviour of a transluminal implant, for instance of an intracoronary implant device, which method comprises computer based analysing of multiple images from in-vivo acquired OCT images, recorded at baseline (freshly implanted device) and at any time point thereafter, of long vessel segments of transluminal implant device formed by strut from bars or of a longitudinal tubular implant device formed by strut from bars in a body vessel, said method comprising: - automatic contouring and identifying structures of the in-vivo acquired images, - segmentation of the implant device and lumen based on A-scan analysis by (1) a bright reflection, (2) a shadow and (3) a rapid rise and fall of energy, - scan conversion of the image to a fast analysis platform, - evaluation of strut apposition or strut coverage from A-line segmentation (A-scan lines) in the scan-converted image, and wherein said method provides automatic identification and measurement of both 1) distance of the separate surfaces zones of said implant device to vessel wall (apposition) and 2) neointima coverage (corresponding to vessel healing after implantation of the implant device). Hereby the segmentation comprises or consists of three steps: (1) pre-processing of the image, (2) identification of candidate A-scan lines, (3) processing of the candidates. Furthermore multiple zone or structure of the implant can be individually analysed for providing such stent strut to vessel wall distance (and neointima coverage) for different individual stent struts zones in the image. Such multiple zones or structures are multiple views or segments of a strut or the multiple zones or structures are multiple images of transversal sections of a strut of the longitudinal tubular implant or the multiple surfaces are formed by at least one axial strut. Such stent struts segmentation is based on A-scan lines analysis whereby a strut in OCT

images is characterized by: (1) a bright reflection (2) a shadow and (3) a rapid rise and fall of energy. Such segmentation can comprise or consist of three steps: (a) pre-processing of the image, (b) identification of candidate A-scan lines, (c) processing of the candidates. Furthermore the pre-processing of images can involve image calibration, whereby the calibration line coincides with the catheter plastic border, whereby using the calibration line as a reference, the catheter can be optionally automatically recognized and ignored from the algorithm for strut segmentation (and lumen segmentation later). In a particular embodiment the A-scan line candidates are identified by searching for strut characteristics whereby the maximum intensity value of each line is located and recorded and if this value exceeds a selected threshold the line is labelled as a candidate. Such A-scan line candidates can be processed by removing the non-desired lines by analysing the shadows coming from a strut and taking into account the depth of the shadow excluding of false candidates (i.e. false candidates because of thrombus, plaque protrusion, blood remnants or other "object" inside the lumen), whereby the intensity level of all the pixels beyond the strut is analysed and the pixels divided into three groups: (1) close to the struts, (2) medium distance and (3) far away whereby the intensity of each group is analysed and if it exceeds a certain fixed value, the candidate is discarded. In a particular embodiment the horizontal coordinates of he located struts are identified by the following steps: 1) the algorithm takes as a starting point the coordinate founded in step b, and from this point, a correction based on intensity level is performed in order to avoid errors resulting from reverberations, blood remnants over the stent (in baseline pullbacks) and misalignment of the coordinates so that the end of this last step, almost all stent struts are correctly segmented avoiding false positive results.

The lumen segmentation can be based on A- scan line analysis consisting of consists of three steps: (1) pre-processing of the image, (2) A-line single analysis and (3) correction considering all A-lines together. Lumen segmentation comprises or consists of three steps: (a) pre-processing of the image, (b) identification of candidate A-scan lines, (c) correction. In a particular embodiment the pre-processing step for lumen segmentation comprises optionally removal of the strut positive A-scan lines which are removed from the image and comprises the three steps (1) based on the histogram of the whole image, turning all the pixels under a selected intensity value are to zero and incrementing all the pixels above another selected fixed value are to a higher intensity. (2) applying a Gaussian symmetric low-pass filter with a 5 pixel

square dimension and sigma equal to 2.5 is applied and (3) morphologically opening the image using a disk structuring element.

EXAMPLES

Example 1: ASSESSMENT OF AREAS AND VOLUMES

1.1. General approach

After lumen borders are fully-automatically traced and stent struts automatically located (previous paragraphs), measurements representing individual stent strut apposition (figure 1A) and neointima coverage (figure 1B) are automatically obtained. From 2D spatial coordinates of stent struts in a single frame, the stent contour is traced interpolating different curves and splines. In case of curves (i.e. ellipse), the mean least square is used to fit the best curve through the stent coordinates (figure 3). The use of splines needs optimization of multiple parameters in order to obtain the correct approximation of the stent contour.

From this data, multiple parameters representing stent apposition, coverage, stent healing and vessel remodelling is assessed, too. Malapposition area and neointimal tissue area is quantified. Analysis of consecutive frames allows for OCT pullback 3D analysis estimating volumes of malapposition and neointimal tissue.

1.2. Stent shape delineation

After segmentation in the polar domain (r,θ), image and relative segmentations are scan-converted to the Cartesian domain (x,y). Within this new domain, the stent shape is re-constructed as follows:

- A set of coordinates, containing the central point of each located strut, is created.
- The best stent-ellipse for the given set of points is estimated.

The second step is obtained through least square optimization extracting ellipse parameters from the conic ellipse equation. Before proceeding with stent contour estimation, the image is analysed to asses if the stent shape can reliably be identified. Inclusion criteria are defined as the following: (1) the image is divided in four quadrants using the centre of mass of the lumen as reference, (2) each quadrant

must contain at least two struts. Frames that do not satisfy these requirements are processed only for individual strut assessment and lumen area.

1.3. Measurements

Measurements are performed in the Cartesian domain after scan conversion to images of pixel dimensions 1024 x 1024. Image quantification is made in two steps:

- strut-by-strut individual apposition/coverage analysis.
- lumen and stent area analysis (including relative difference) and, consecutively, assessment of volume representing distance between tissue wall and stent (or volume of neo-intimal tissue in case of follow-up datasets).

Strut-by-strut individual quantification is obtained as follows: from the strut central point, the minimum distance perpendicular to the lumen segmentation is computed. If more than one direction is perpendicular to the vessel boundary (in case of high curvature), the minimal distance is taken. In this way it is possible to reliably assess strut apposition/coverage also in case of sunflower artefact (when due to eccentric catheter position stent struts surface appear rotated towards the catheter) (figure 6). Discrimination between apposed/malapposed struts is obtained applying the following threshold [2]: T = real strut thickness + polymer thickness (in case of drug eluting stent) + blooming artefact. If the measured strut/lumen distance in inferior to T, the relative strut is labelled as apposed, otherwise it is labelled as malapposed. In the same way it is possible to discriminate between covered/uncovered struts. In this last case the threshold is taken equal to 20μm.

Lumen area (L_A) is obtained through numerical trapezoidal integration of the *lumen-spline*. Stent area (S_A) is computed with the equation of the area of the ellipse.

Apposition area (AA) and neointimal tissue area (NTA) is obtained computing the "positive" difference between L_A and S_A (figure 2): intersection points between the two curves are identified and areas divided into different sectors. In the case of freshly implanted stents, the sum of sectors where the difference between lumen area and stent area is positive, represents apposition area (AA). For follow-up databases, neo-intimal tissue area (NTA) is represented by the sum of sectors where the difference between stent area and lumen area (opposite as previous) is positive.

Volumetric quantification is then be obtained estimating AA (or NTA) through consecutive slices cross images). Given that, the IV-OCT system acquires slices at a predefined speed and frame rate, the distance between adjacent slice is constant (i.e. 0.03 mm). Multiplying AA (NTA, L_{Area}, S_{Area}) values of consecutive slices by their relative longitudinal slice distance allows for estimation of lumen, stent and apposition/neointimal-tissue volumes.

Apposition volume represents the space between vessel wall and stent surface, neo-intimal tissue volume the amount of tissue growth over the stent surface (figures 4 and 5).

1.4. Validation and Results

Validation was performed by evaluating a test set of 108 *in-vivo* images randomly selected from 9 different *in-vivo* pullbacks. Areas analysis was performed manually by two trained cardiologists and by the automated procedure. Regression analysis was performed and correlation between the manual and the automatic measurements was expressed using the Pearson's correlation coefficient. Agreement between both measurements was assessed through Bland-Altman analysis.

Area quantification, both for lumen and stent, regression analysis showed a correlation coefficient of 0.99, while Bland-Altman statistics do not show any significant bias (figure 7).

Example 2: REGISTRATION

Registration of pullbacks of the OCT catheter which creates cross sectional images of the same vessel (e.g. vascular vessel) at different times will allow the users to directly follow the vessel healing process, after stent implantation, comparing corresponding frames at different time intervals (e.g. baseline, 3 months, 6 months and 9 months).

Registration of stented segments is done through automatic identification of stent strut coordinates. As soon as two pullbacks of the same stented vessel at different times are analysed, as previously reported, position of stent struts in 3D space is available. Then a reconstruction of the stent structure is computed and represented (figure 8). Starting from these data, the algorithm for registration of clouds of points (for example ICP, iterative closest points) can compute the transformation able to match the two clouds. Registration results will allow the user to compare corresponding frames at different times. Assessment on how human coronary arteries react at implantation of different kinds of stents and drug treatments is of vital importance for clinicians and stent manufacturers.

2.1. OCT dataset alignment

As a first step, 3D structures must be automatically aligned: same centre and same long-axis direction. Centre of mass of both OCT pullbacks are computed using the strut coordinates as a system of particles:

$$C_M = \frac{\sum_{i=1}^{N} m_i r_i}{\sum_{i=1}^{N} m_i}$$

setting the mass of all the strut particles equals to 1. 3D datasets can then be shifted through the 3D space in order to match the two centres of mass (figure 9).

The moments of inertia of the two objects are then computed and the 3D datasets consecutively aligned in the long-axis direction (z). Moment of inertia of a rigid object of N point masses m_i is computed in the following way:

$$I = \begin{matrix} I_{11} & I_{12} & I_{13} \\ I_{21} & I_{22} & I_{23} \\ I_{31} & I_{32} & I_{33} \end{matrix}$$

With:

$$I_{11} = \sum_{i=1}^{N} m_i(y_k^2 + z_k^2) \quad I_{22} = \sum_{i=1}^{N} m_i(x_k^2 + z_k^2) \quad I_{33} = \sum_{i=1}^{N} m_i(x_k^2 + y_k^2)$$

$$I_{12} = -\sum_{i=1}^{N} m_i x_k y_k \quad I_{13} = -\sum_{i=1}^{N} m_i x_k z_k \quad I_{23} = -\sum_{i=1}^{N} m_i y_k z_k$$

Through the Eigen vectors of matrix I, it is possible to correctly align the two datasets in the long axis direction (figure 10).

2.2. Object rotation

After matching the centres of mass and aligning the two datasets in the long-axis direction, correct 3D rotation is estimated through the use of cost function. Given that p_i represent a point in the Euclidean space and S a surface in the same space, the distance between p_i and S is defined as:

$$f_{dist}(p_i, S) = \min(\|p_i - p_s\|^2) \quad \forall p_s \in S$$

From this, we can define a cost function between two surfaces S_1 and S_2 as follows:

$$f_{cost}(S_1, S_2) = \frac{1}{N}\sum_{i=1}^{N}(f_{dist}(p_i, S_1))^2 \quad \forall p_i \in S_2$$

with N the number of points belonging to S_2.

Iteratively rotating S_2 of a predefined small angle α (i.e. 2°) from 0° to 360° and computing $f_{cost}(S_1,S_2)$ at every step, the cost function gives information about the distance between the two objects for every possible rotation (figure 11). Minimization of the cost function f_{cost} will result in the rotation able to match the two 3D objects (figure 12).

2.3. Iterative Closest Points (ICP)

After minimization of the cost functions, registration between the two clouds of points is refined through algorithms for difference minimization. Through ICP (iterative closest points), the two clouds is finally matched computing the refined

transformation (figure 13). Points reported in paragraph 2.1 and 2.2 (pre-ICP registration) avoid ICP to stop at local minima.

2.4. Final output

Final output of the registration procedure (figure 14) is the transformation (rotation, translation) able to match the two pullbacks: translation matrix, rotation matrix (rototranslation matrix) are the outputs.

Through the use of an automated mask, strut shadows, catheter, guide-wire shadow and brightness is correctly removed from analysis. Then the intensity level between two images is used to further refine registration in the long-axis direction (z) or even in a 2D space. Finally, to obtain even more accurate results, the two datasets is divided into multiple different sectors (multi resolution registration or local level registration)and the above procedure applied to every sector.

Results of the registration is used to compare 3D intravascular OCT datasets frame-to-frame (figure 14).

Example 3: Malapposition and Coverage Clustering method

3.1. General Approach

A method of present invention able to appreciate malapposition as a volume, and not every strut individually, is the clustering of malapposed struts according to their spatial 3D location. Malapposed struts are divided into different groups and for every group relevant properties is quantified. The proposed method concerns completely automatic detection (segmentation) of stent struts and lumen for each frame. Consecutively, discrimination of apposed from malapposed struts is obtained with the use of a threshold computed as follows:

A_T (apposition threshold) = strut thickness + polymer thickness (in case of drug eluting stents) + blooming artefacts.

If strut individual apposition > A_T the strut is labelled as malapposed, otherwise apposed. Such method results in 3D position of every strut and discrimination between apposed and malapposed struts.

3.2. Clustering

Malapposed and uncovered struts are clustered into different groups according to their 3D position in space (figure 15). Then, for every cluster, properties like relative long-axis position, length in long-axis direction, angle distribution, number of struts belonging to the group and maximum, minimum and mean strut malapposition values is quantified. In addition, general results (of the whole stented sector) about the number and percentage of apposed and malapposed struts, number of embedded and protruding struts, number of isolated malapposed struts and clusters is consecutively obtained.

Moreover, as a first end-point, for every located cluster, the volume of the whole malapposition (i.e. space between stent to vessel wall) and/or neointimal coverage is quantified with the methods reported at paragraph 1.2 and 1.3.

3.3. Clustering algorithm

Clustering is a technique which aims to define groups of variables with homogenous properties within the group they belong to and inhomogeneous properties between other groups. In order to cluster malapposed and uncovered struts, non-supervised

clustering techniques based on distance measurements is used. Clusters are defined through a hierarchical agglomerative clustering algorithm composed of three steps (figure 16):

(1) Definition of a distance measure, for example Euclidean distance:

$$d_{xy} = \left[\sum_{i=1}^{m} (s_i - s_j)^2\right]^{1/2}$$

where $s_i(x,y,z)$ and $s_j(x,y,z)$ are two elements in Cartesian space with z representing long-axis position. Other kinds of distance, like Mahalanobis or city-block, is used instead of the simplest Euclidean distance.

(2) Computation of the pair-wise distance matrix D between all the elements.

(3) Iterative fusion of the 2 most similar elements in a cluster and updating of matrix D. An appropriate method for update is Single Linkage (SL) also called *nearest neighbour*. SL uses the smallest distance between objects in two clusters to update the matrix mathematically:

$$D(X,Y) = \min(d(x,y))$$

where X and Y are the two clusters, D(X,Y) distance between the two clusters and d(x,y) distance between elements $x \in X$ and $y \in Y$.

As every hierarchical clustering procedure, such algorithm produces as output a *hierarchical tree* which starts from *leaves* (single strut) and ends into a super-cluster containing all the struts. Such a tree is obtained through subsequent fusion of elements in clusters becoming bigger step by step (agglomerative methods). The number of the clusters is dependent on the level at which the tree is observed. The final choose of the number of clusters is done manually (pre-setting at which level the tree is observed) by the user or through a cut-off value.

The proposed methods for clustering of malapposition are applied also to uncovered struts (clustering of uncovered strut) in case of stent coverage assessment. This allows for assessment of strut coverage through 3D space, quantifying the volume of neo-intimal tissue growth on top of stent surface.

Particular and preferred aspects of the invention are set out in the accompanying independent and dependent claims. Features from the dependent claims may be combined with features of the independent claims and with features of other dependent claims as appropriate and not merely as explicitly set out in the claims.

Thus, the claims following the detailed description are hereby expressly incorporated into this detailed description, with each claim standing on its own as a separate embodiment of this invention.

Drawing Description

BRIEF DESCRIPTION OF THE DRAWINGS

The present invention will become more fully understood from the detailed description given herein below and the accompanying drawings which are given by way of illustration only, and thus are not limitative of the present invention, and wherein:

Figure 1 provides examples of individual strut segmentation & quantification, lumen contouring and lumen area quantification. Panel A contain an example of apposition analysis, panel B of coverage analysis.

Figure 2: provides an example of lumen and stent-ellipse overlapping. In order to correctly estimate apposition and neo-intimal tissue area, discrimination of sectors where lumen area is bigger than stent area, and opposite case, is needed.

Figure 3: provides lumen and stent segmentation (Panels A and B) and examples of tracing of stent contour (Panels C and D)

Figure 4 is a graphic display with left panel: malapposition area assessment (in purple or [A] in figure). Right panel: neointimal tissue area assessment (in green or [B] in figure).

Figure 5 neointimal tissue area assessments (in green in figure [B]).

Figure 6 is a graphic of a stent strut assessment in case of sunflower artefacts

Figure 7 provides graphics that demonstrate the area assessment validation

Figure 8 provides a figure which contains two unregistered 3D stent

Figure 9 is a graphic display of 3D stent after centre of mass alignment

Figure 10 is a graphic display of moment of inertia in the long-axis direction z (in green or [C] in figure).

Figure 11 is a graphic display of cost function for correct rotation

Figure 12 is a graphic display of 3D stent after alignment and rotation

Figure 13 is a graphic display of refining of the registration results after clouds matching (algorithm likes icp)

Figure 14 is a graphic display of frame-to-frame registration results to compare same vessel after different instants of time.

Figure 15 provides an example of malapposition clustering. Colored dots (or different grey tone) correspond to malapposed struts, different colour to different clusters. Blue line ([D]) is a reference starting and ending on the two edges of the stent.

Figure 16 is a graphic display of hierarchical agglomerative clustering: five steps iterative procedure for a six elements database. At every step the distance matrix and the hierarchical tree are computed (red number correspond to the length of the branches); figure also illustrates how elements are merged into different clusters.

AUTOMATIC VOLUMETRIC ANALYSIS AND 3D REGISTRATION OF CROSS SECTIONAL OCT IMAGES OF A STENT IN A BODY VESSEL

Claims

1. A computer based method of automated volumetric (3D) stent analysis and OCT datasets registration comprising computer based analysis of multiple consecutives images from in-vivo acquired cross sectional OCT images, recorded by an OCT catheter pullback at baseline (freshly implanted device) and at any time point thereafter, of long vessel segments of stent formed by strut from bars in a body vessel (e.g. vascular) the method comprising automatic structures identification and segmentation (e.g. vessel wall and stent), distance identification and measurement of the separate surfaces zones of said implant device to vessel wall (apposition) and/or covering neointima (corresponding to vessel healing after implantation of the implant device) and the method being

characterised in that

1) individual stent strut coverage/apposition and further areas and volumes of separate surfaces zones of a) said implant device to vessel wall (apposition) or b) of neointima coverage are volumetric measured by automatic clustering of covered/uncovered stent struts according to their spatial 3D location through analysis of equally spaced consecutive OCT cross sectional images and/or by automatically clustering apposed/malapposed struts according to their 3D spatial position through consecutive cross sectional images and

2) landmark based registration (e.g. using stent struts position as landmarks) of intravascular OCT datasets of same vessel at different time points of the implantation period comprising a) 3D alignment by rotation and translation and b) refinement of the registration by iterative algorithms (e.g. Interactive closest point (ICP)) and c) multi dimensional registration (i.e. local level) for best accuracy.

2. The method according to claim 1, whereby malapposition is measured as a volume and not only as every strut individually (clustering of malapposed struts according to their spatial 3D location to measure).
3. The method according to any one of the claims 1 to 2, whereby malapposed struts are divided into different groups and for every group relevant properties are quantified.
4. The method according to any ones of the previous claims, whereby for each frame the proposed method concerns completely automatic detection (segmentation) of stent struts and lumen and consecutively, discrimination of apposed from malapposed struts is obtained with the use of a threshold computed as A_T (apposition threshold) = strut thickness + polymer thickness (in case of drug eluting stents) + blooming artefacts whereby if strut individual apposition > A_T the strut is labelled as malapposed, otherwise apposed such that 3D position of every strut and discrimination between apposed and clustered malapposed struts is obtained.
5. The method according to claim 1, whereby malapposed struts are into different groups according to their 3D position in space and consequently for every cluster, properties like relative long-axis position, length in long-axis direction, angle distribution, number of struts belonging to the group and maximum, minimum and mean strut malapposition values is quantified
6. The method according to claim 5, whereby of a stented sector the number and percentage of apposed and malapposed struts, the number of embedded and protruding struts and/or the number of isolated malapposed struts and clusters is measured.
7. The method according to any one of the claims 1 to 6, whereby as a first end-point, for every located cluster, the volume of the whole malapposition (i.e. space between stent to vessel wall) is quantified by 1) stent shape delineation and 2) scan conversion to pixels followed by image quantification involving a) strut by strut individual apposition and/or neointima coverage analysis and b) lumen area and/or stent area analysis and 3) computing the relative difference between lumen area and stent area and 3) volumetric quantification of the apposition area and/or neointimal tissue area through consecutive cross sectional images for volume estimation lumen volume, stent volume and the apposition volume or neointimal tissue volume

8. The method according to any one of the previous claims, whereby the algorithmic clustering technique is adapted to define groups of variables with homogenous properties within the group they belong to and inhomogeneous properties between other groups.
9. The method according to claim 8, whereby the algorithmic clustering technique is non-supervised clustering techniques based on distance measurements (in order to cluster malapposed struts) whereby clusters are defined through a hierarchical agglomerative clustering algorithm composed of three steps (1) definition of a distance measure (for example Euclidean distance), (2) computation of the pair-wise distance matrix D between all the elements and (3) iterative fusion of the 2 most similar elements in a cluster and updating of matrix D (e.g. Single Linkage (SL)).
10. The method according to any one of the previous claims 8 to 9, whereby the algorithm produces as output a *hierarchical tree* which starts from *leaves* (single strut) and ends into a super-cluster containing all the struts of an analysed long vessel zone of a stent in a body vessel.
11. The method according to claim 10, whereby the *hierarchical tree* is obtained through subsequent fusion of elements in clusters becoming bigger step by step (agglomerative methods) and whereby the number of the clusters is dependent on the level at which the tree is observed.
12. The method according to claim 11, whereby the final choose of the number of clusters is carried out manually (pre-setting at which level the tree is observed) by the user
13. The method according to claim 11, whereby the final choose of the number of clusters is through a cut-off value.
14. The method according to any one of the previous claims whereby stent strut coordinates of two pullbacks of the same stented vessel at different times and the position of stent struts in 3D space and a reconstruction of the stent structure as clouds of points is computed and starting from these data match the two clouds by an algorithm for registration of clouds of points (for example ICP, iterative closest points).
15. The method according to any one of the previous claims whereby OCT alignment of a dataset of two pullbacks of the same stented vessel at different times comprises a first

step of computing 3D structures aligned according to same centre and same long-axis direction

16. The method according to claim 15, whereby the centre of mass of both OCT pullbacks are computed using the strut coordinates as a system of particles according to the following function:

$$C_M = \frac{\sum_{i=1}^{N} m_i r_i}{\sum_{i=1}^{N} m_i}$$

setting the mass of all the strut particles equals to 1.

17. The method according to claim 16, whereby the 3D datasets is consequently shifted through the 3D space in order to match the two centres of mass and the moments of inertia of the two objects are then computed and the 3D datasets consecutively aligned in the long-axis direction (z).

18. The method according to claim 17, whereby the moment of inertia of a rigid object of N point masses m_i is computed in the following matrix:

$$I = \begin{matrix} I_{11} & I_{12} & I_{13} \\ I_{21} & I_{22} & I_{23} \\ I_{31} & I_{32} & I_{33} \end{matrix}$$

with:

$$I_{11} = \sum_{i=1}^{N} m_i (y_k^2 + z_k^2) \quad I_{22} = \sum_{i=1}^{N} m_i (x_k^2 + z_k^2) \quad I_{33} = \sum_{i=1}^{N} m_i (x_k^2 + y_k^2)$$

$$I_{12} = -\sum_{i=1}^{N} m_i x_k y_k \quad I_{13} = -\sum_{i=1}^{N} m_i x_k z_k \quad I_{23} = -\sum_{i=1}^{N} m_i y_k z_k$$

19. The method according to claim 17, whereby the two datasets through the Eigen vectors of matrix I are aligned in the long axis direction.

20. The method according to any one of the claims 15 to 20, whereby after matching the centres of mass and aligning the two datasets in the long-axis direction, correct 3D rotation is estimated through the use of cost function.

21. The method according to claim 20, whereby the cost function is defined between two surfaces S_1 and S_2 as follows:

$$f_{cost}(S_1,S_2)=\frac{1}{N}\sum_{i=1}^{N}(f_{dist}(p_i,S_1))^2 \quad \forall p_i \in S_2$$

with N the number of points belonging to S_2 whereby p_i represent a point in the Euclidean space and S a surface in the same space, the distance between p_i and S is defined as:

$$f_{dist}(p_i,S)=\min(\|p_i-p_s\|^2) \quad \forall p_s \in S$$

and whereby iteratively rotating S_2 of a predefined small angle α (i.e. 2°) from 0° to 360° and computing $f_{cost}(S_1,S_2)$ at every step, the cost function gives information about the distance between the two objects for every possible rotation (figure 11) and whereby minimization of the cost function f_{cost} will result in the rotation able to match the two 3D objects.

22. The method according to any one of the previous claims, whereby after minimization of the cost functions, registration between the two clouds of points is refined through algorithms for difference minimization.
23. The method according to any one of the previous claims, whereby through ICP (iterative closest points), the two clouds is finally matched computing the refined transformation.
24. The method according to claim 23, whereby a an output of translation matrix and rotation matrix (rototranslation matrix) is provided.
25. The method according to any one of the previous claims 23 to 24, providing further refining through an accurate use of intensity level registration methods (i.e. mutual information, cross correlation).
26. The method according to any one of the previous claims 23 to 25, whereby catheter and catheter shadow or guide-wire shadow and brightness (guide-wire artefact) is additionally removed from analysis through the use of an automated mask and area constrains.
27. The method according to any one of the previous claims 23 to 26, whereby to obtain even more accurate results, the two datasets is divided into multiple different sectors and the above procedure applied to every sector.
28. The use of the method according to any one of the previous claims to compare 3D intravascular OCT datasets frame-to-frame (i.e. on an image level).

29. The use of the method of any one of the previous claims on pullbacks of the same vessel at different intervals (e.g. baseline, 3 months, 6 months, 9 months 12 months, 16 months or more) to measure or follow the vessel healing process, after stent implantation, comparing corresponding frames at the different time intervals (e.g. baseline, 3 months, 6 months and 9 months, 12 months, 16 months or more).
30. The use of the method of any one of the previous claims to compare corresponding frames at different times to assessment on how human coronary arteries react at implantation of different kinds of stents.
31. The use of the method of any one of the previous claims to compare corresponding frames at different times to diagnose how human coronary arteries react after stent implantation on drug treatments.
32. An OCT apparatus with a processor adapted to receive input signals generated by pullbacks of an OCT catheter whereby the processer comprises an algorithm to carry out data processing according to any one of the previous claims 1 to 27.

FIGURES

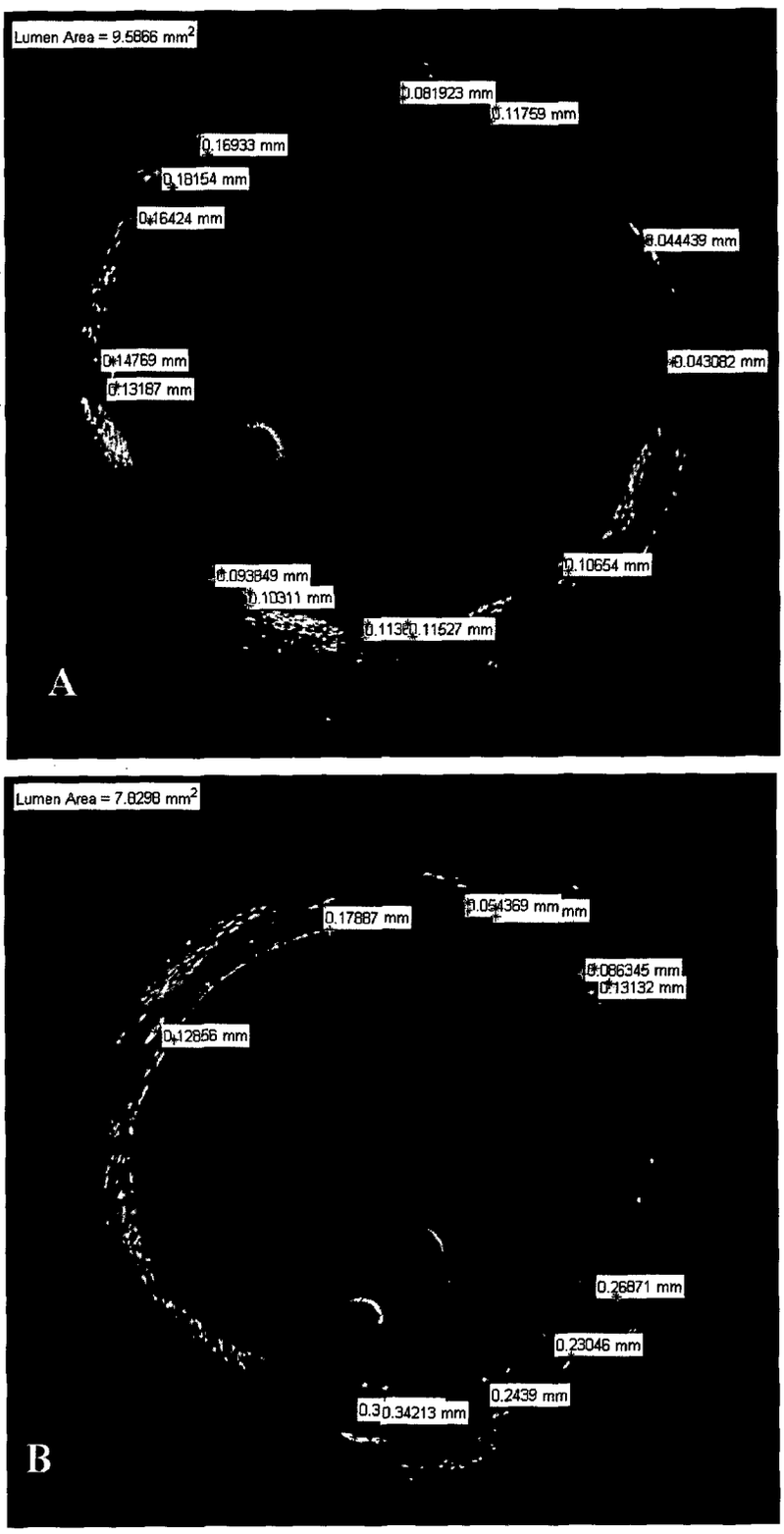

Figure 1

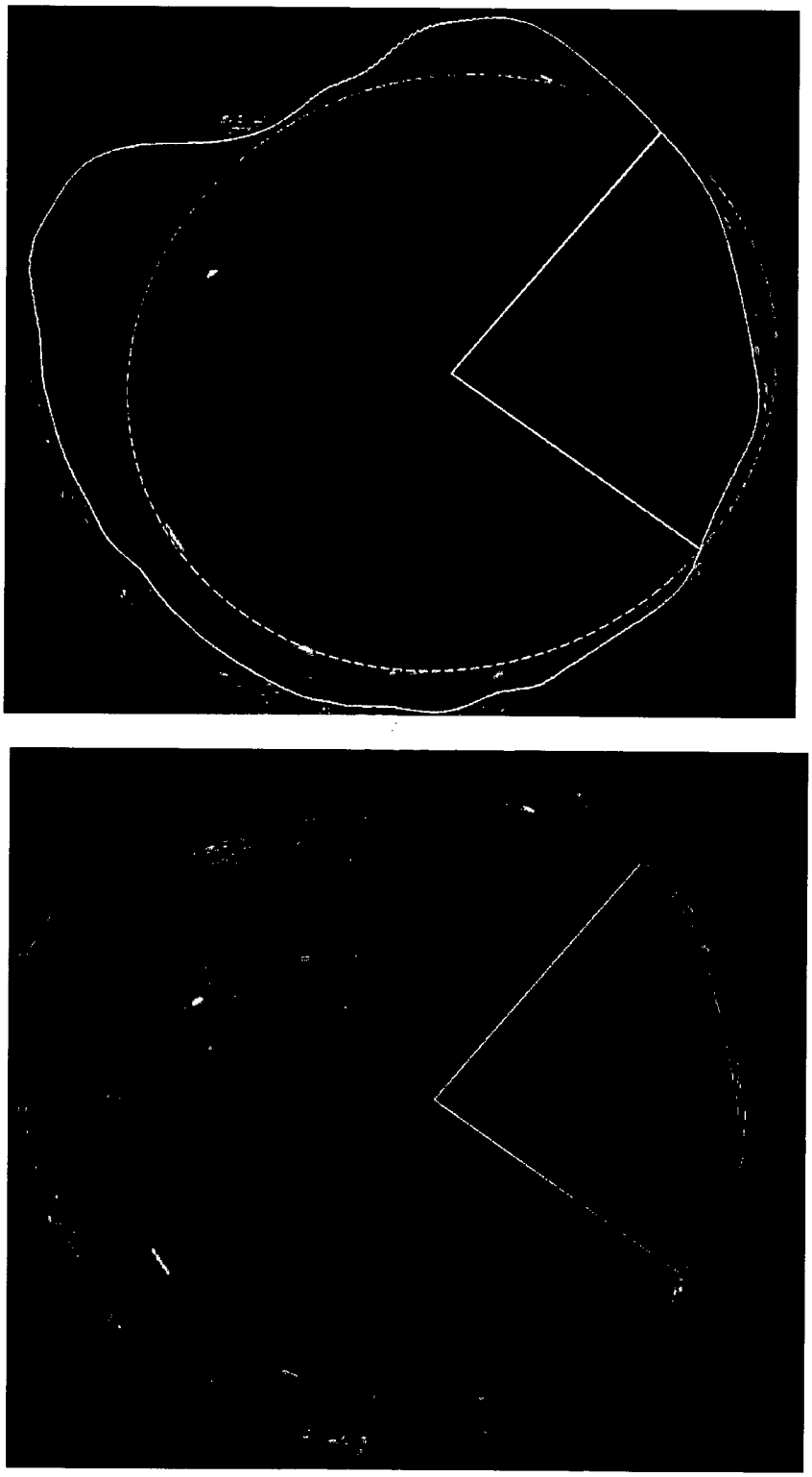

Figure 2

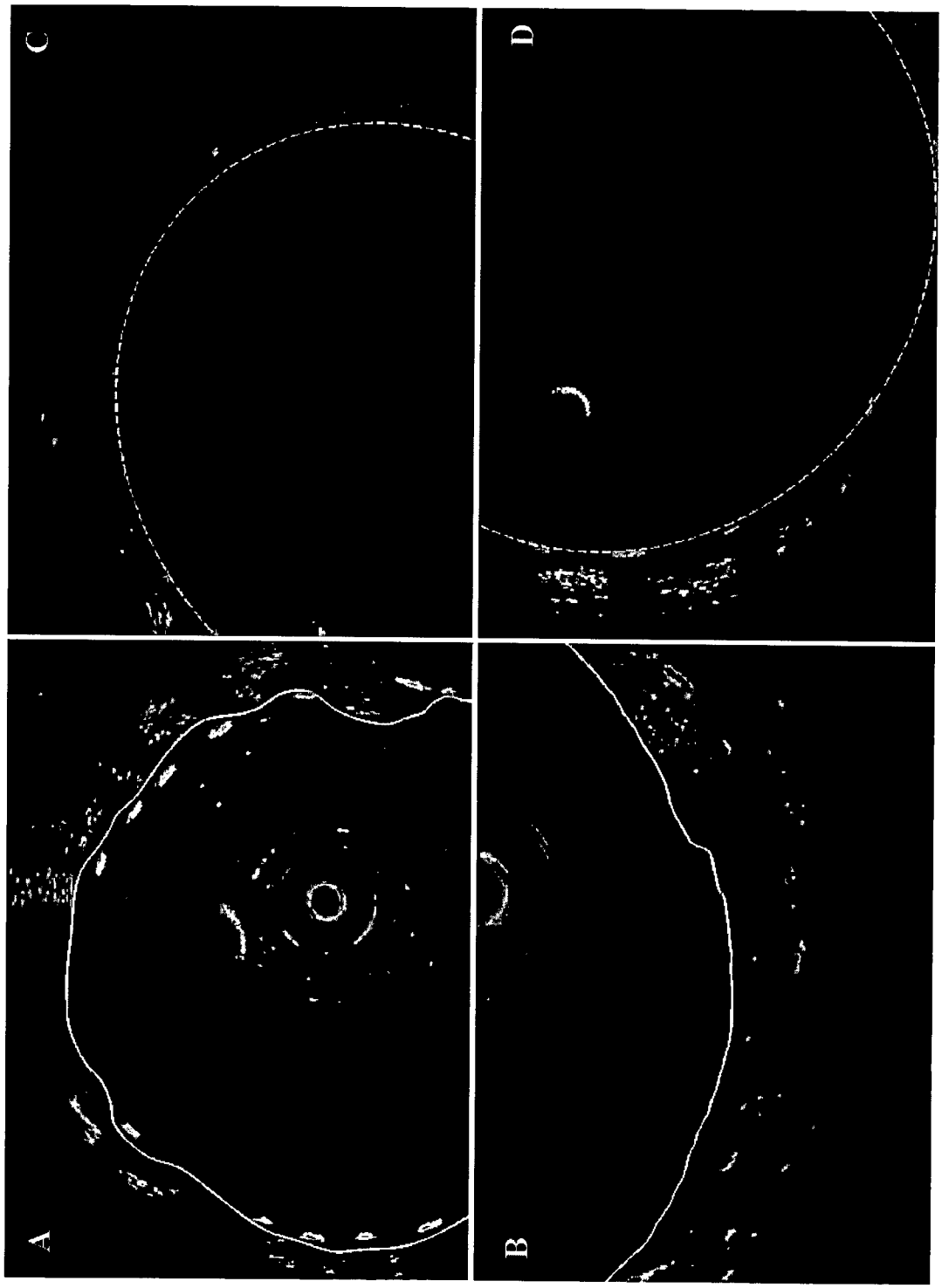

Figure 3

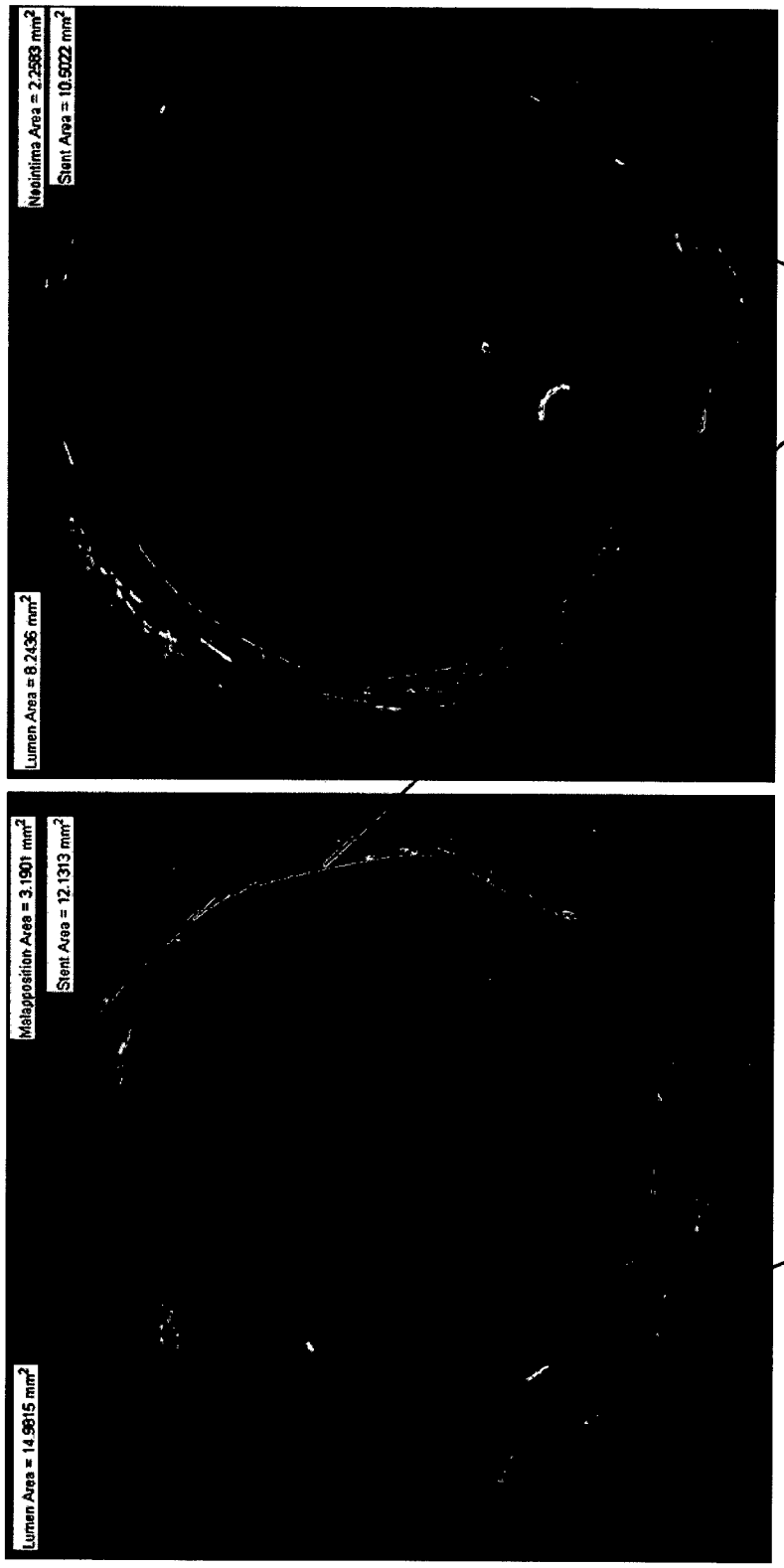
Neointima Area = 2.2583 mm²
Stent Area = 10.5022 mm²
Lumen Area = 8.2436 mm²
Malapposition Area = 3.1901 mm²
Stent Area = 12.1313 mm²
Lumen Area = 14.9815 mm²
A
B

Figure 4

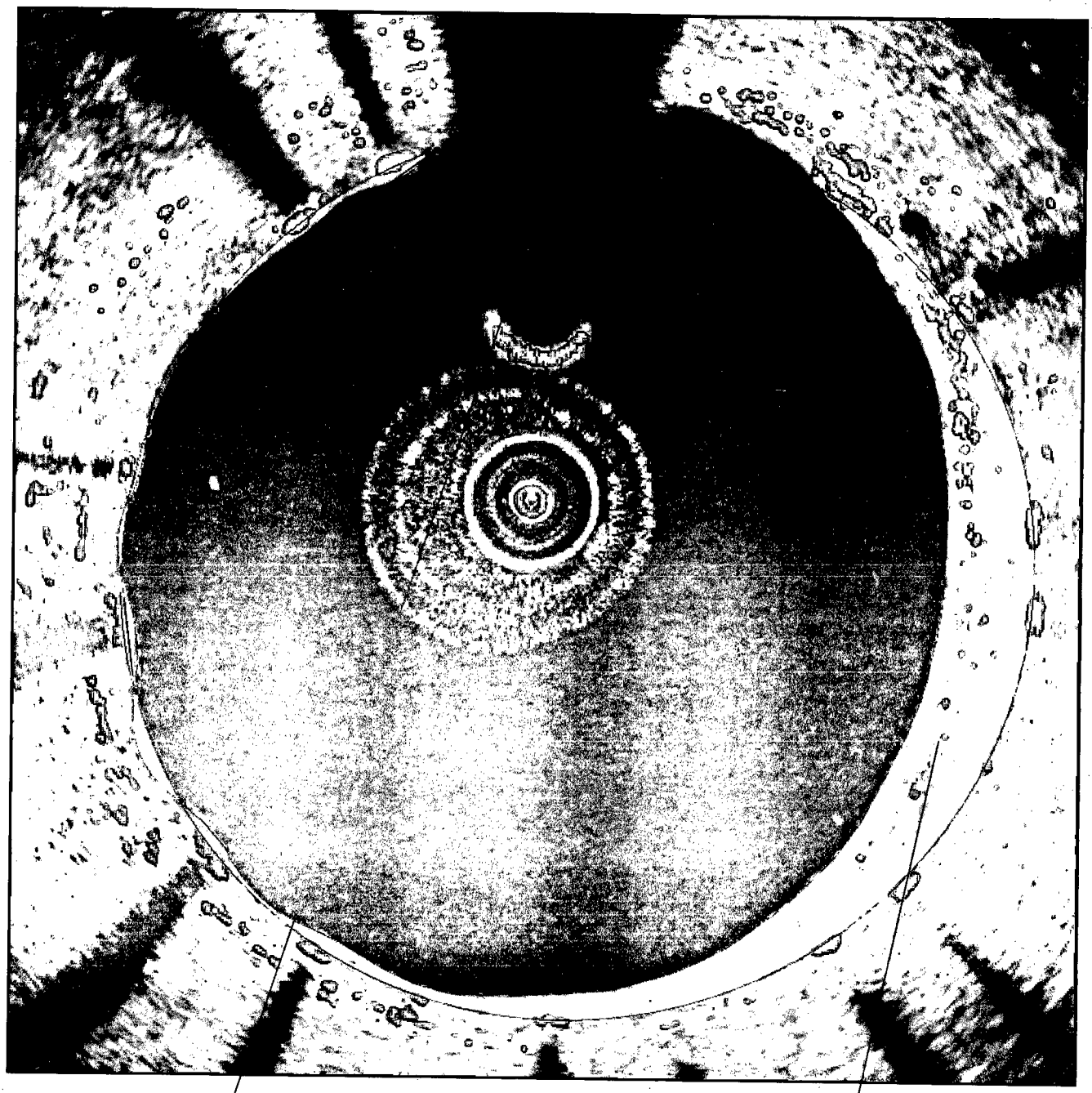

Figure 5

A

B

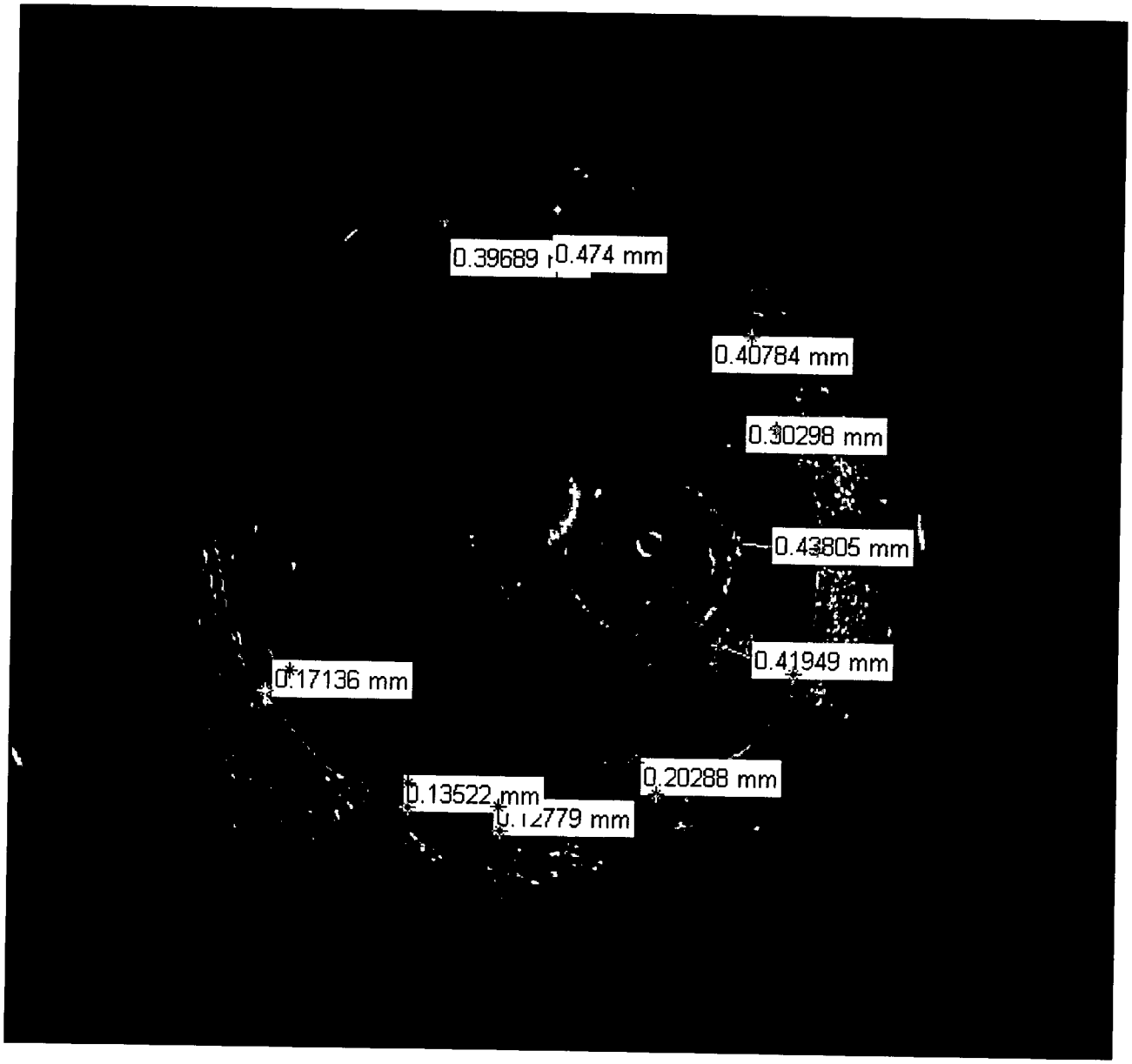
0.39689
0.474 mm
0.40784 mm
0.30298 mm
0.43805 mm
0.41949 mm
0.17136 mm
0.20288 mm
0.13522 mm
0.12779 mm

Figure 6

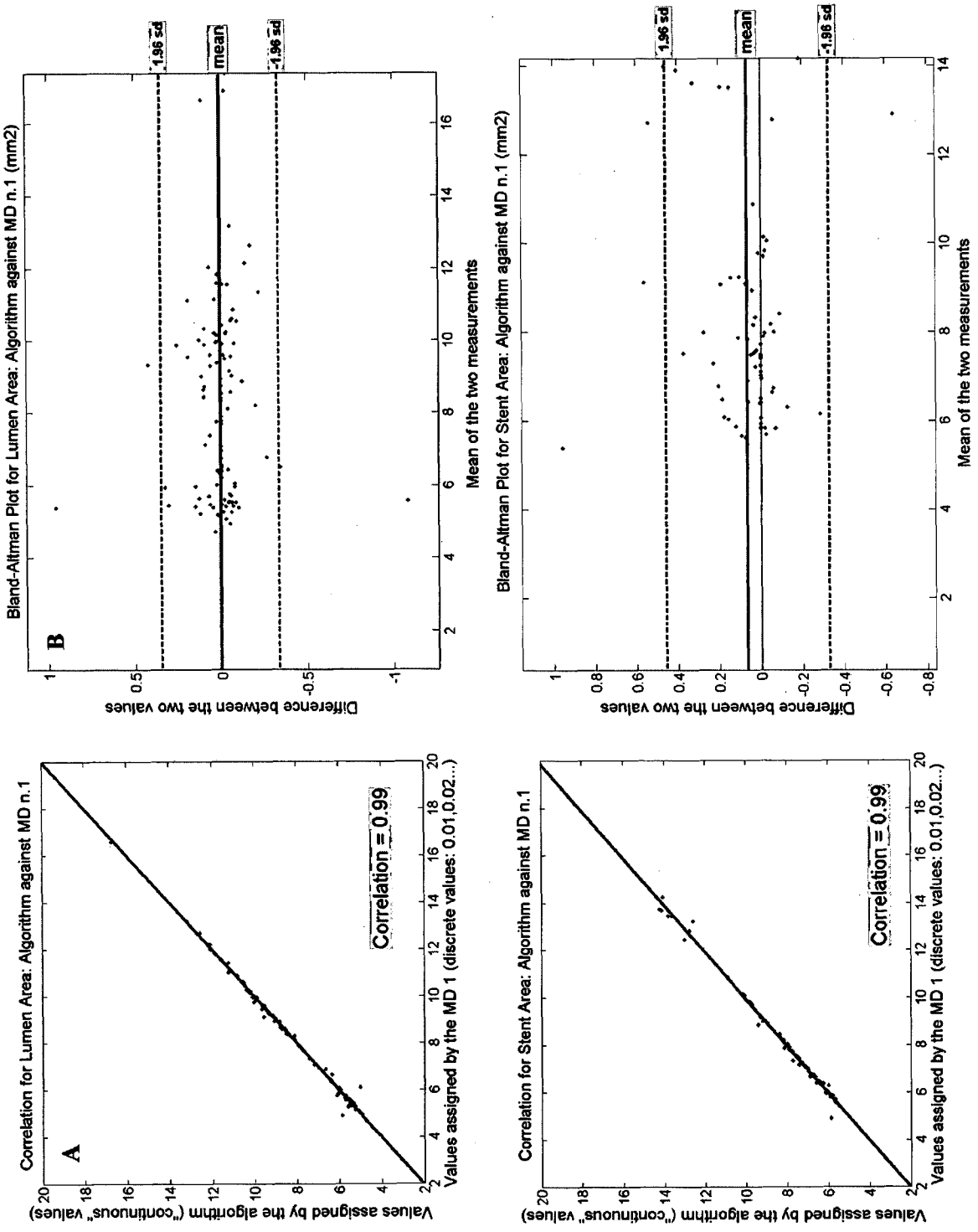
A
Correlation for Lumen Area: Algorithm against MD n.1
Correlation = 0.99
Values assigned by the algorithm ("continuous" values)
Values assigned by the MD 1 (discrete values: 0.01,0.02...)
B
Bland-Altman Plot for Lumen Area: Algorithm against MD n.1 (mm2)
1.96 sd
mean
-1.96 sd
Difference between the two values
Mean of the two measurements
Correlation for Stent Area: Algorithm against MD n.1
Correlation = 0.99
Values assigned by the algorithm ("continuous" values)
Values assigned by the MD 1 (discrete values: 0.01,0.02...)
Bland-Altman Plot for Stent Area: Algorithm against MD n.1 (mm2)
1.96 sd
mean
-1.96 sd
Difference between the two values
Mean of the two measurements

Figure 7

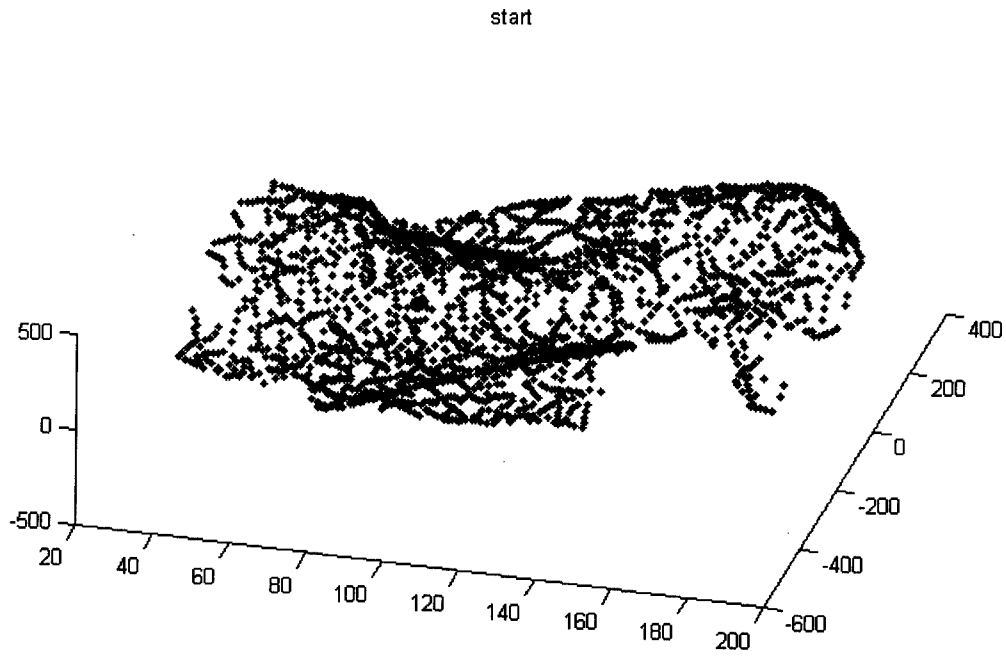

Figure 8

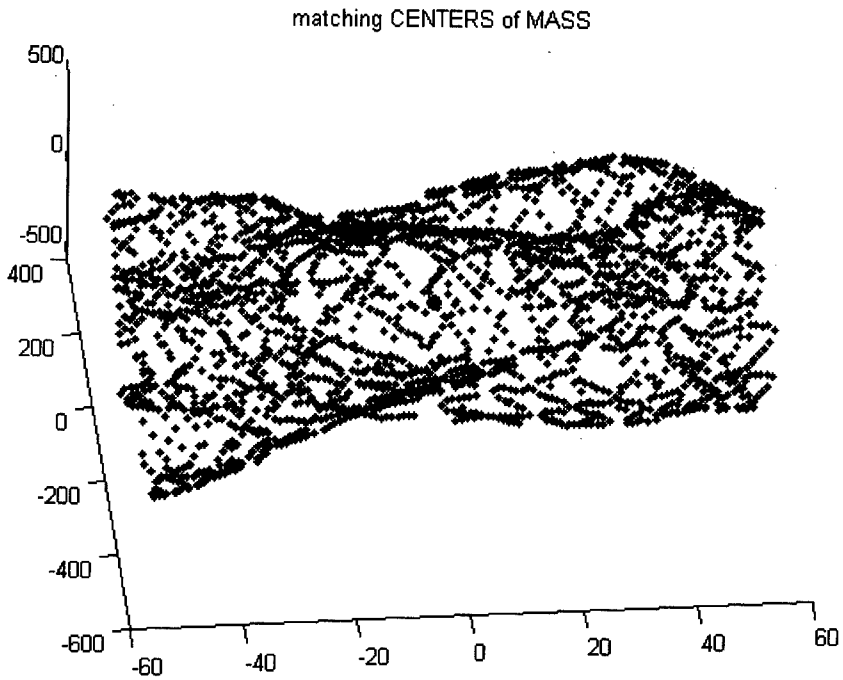

Figure 9

Figure 10

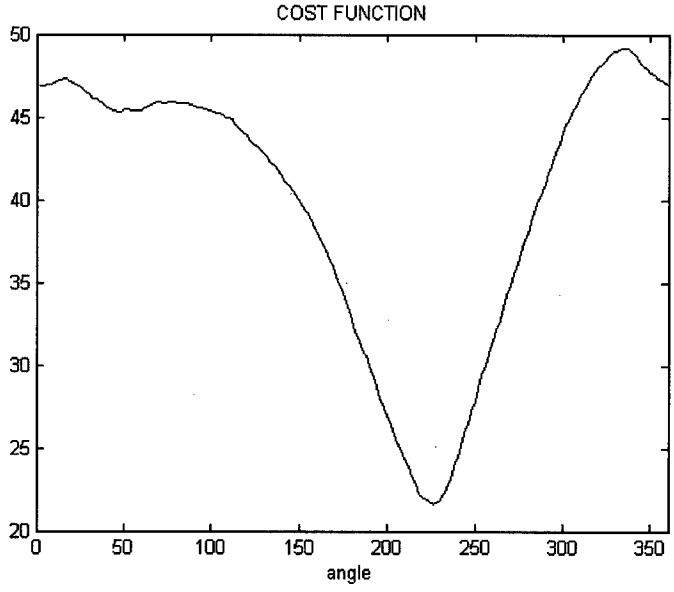

Figure 11

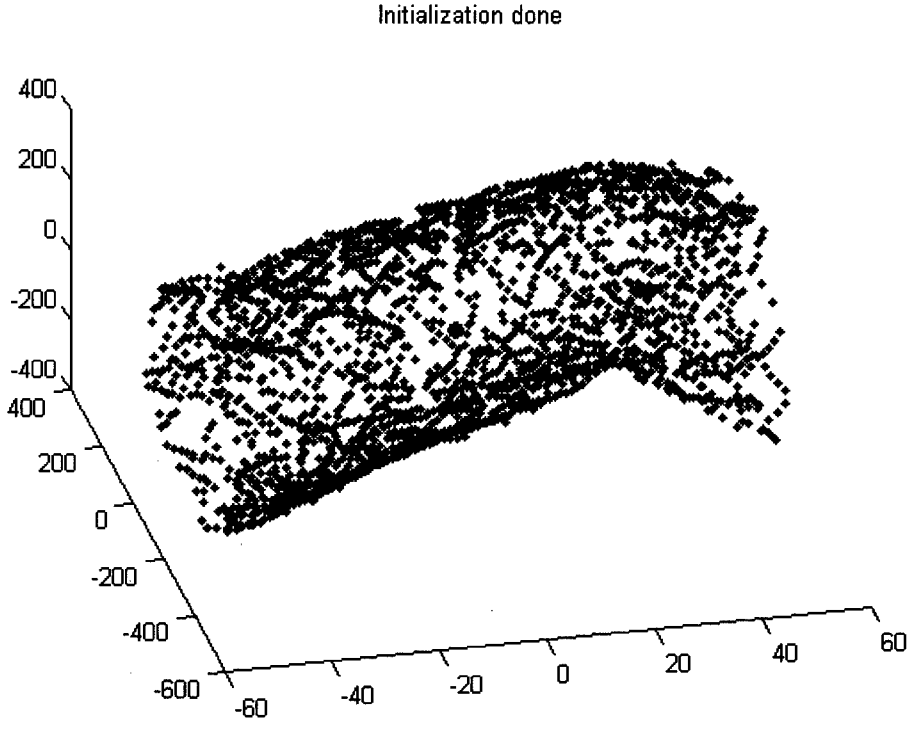

Figure 12

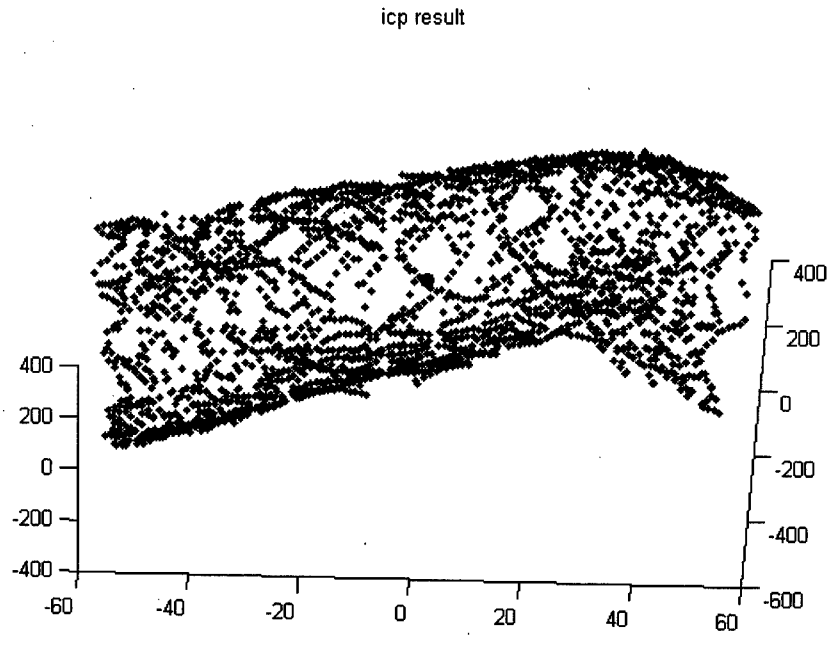

Figure 13

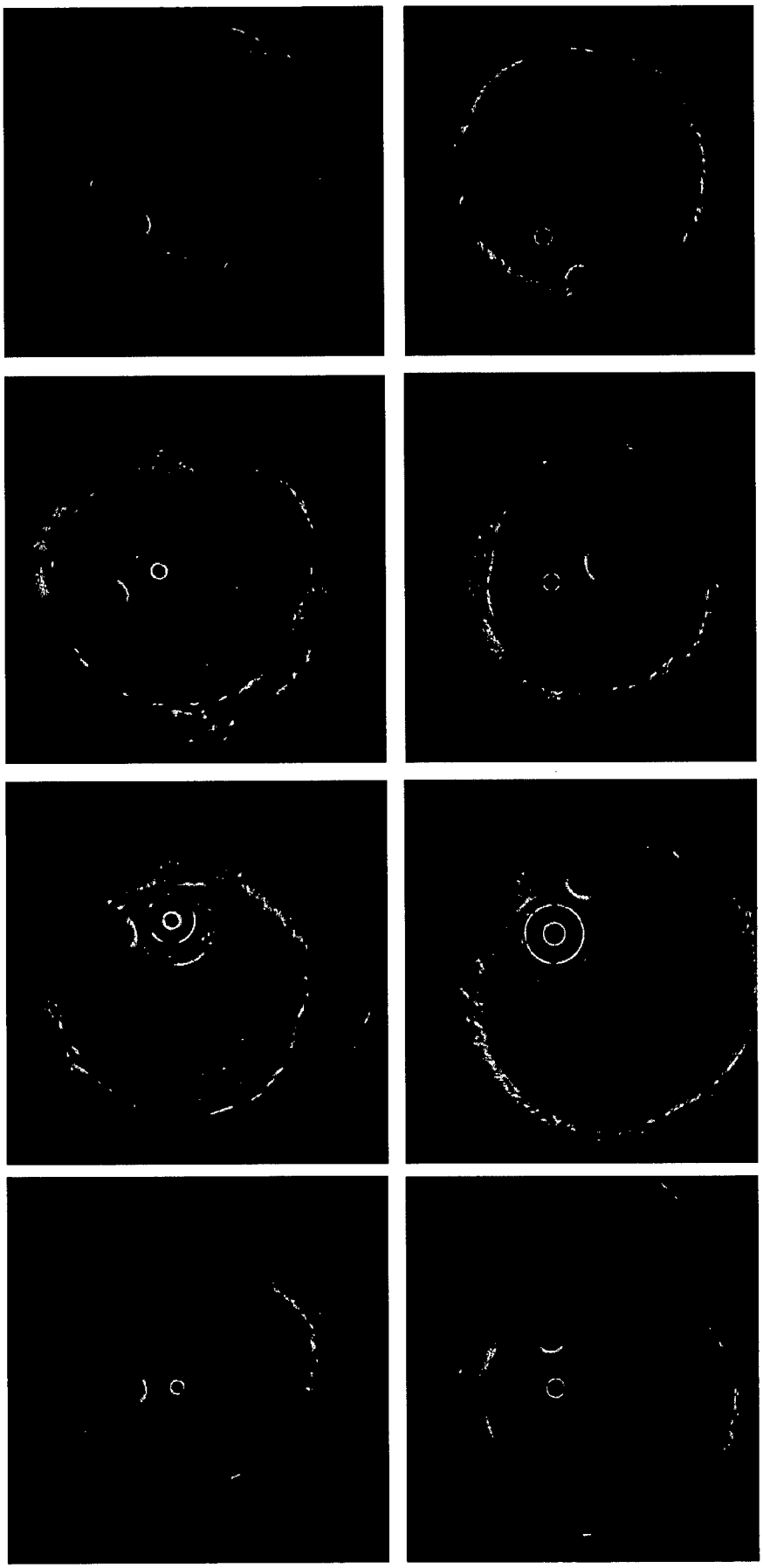

Figure 14

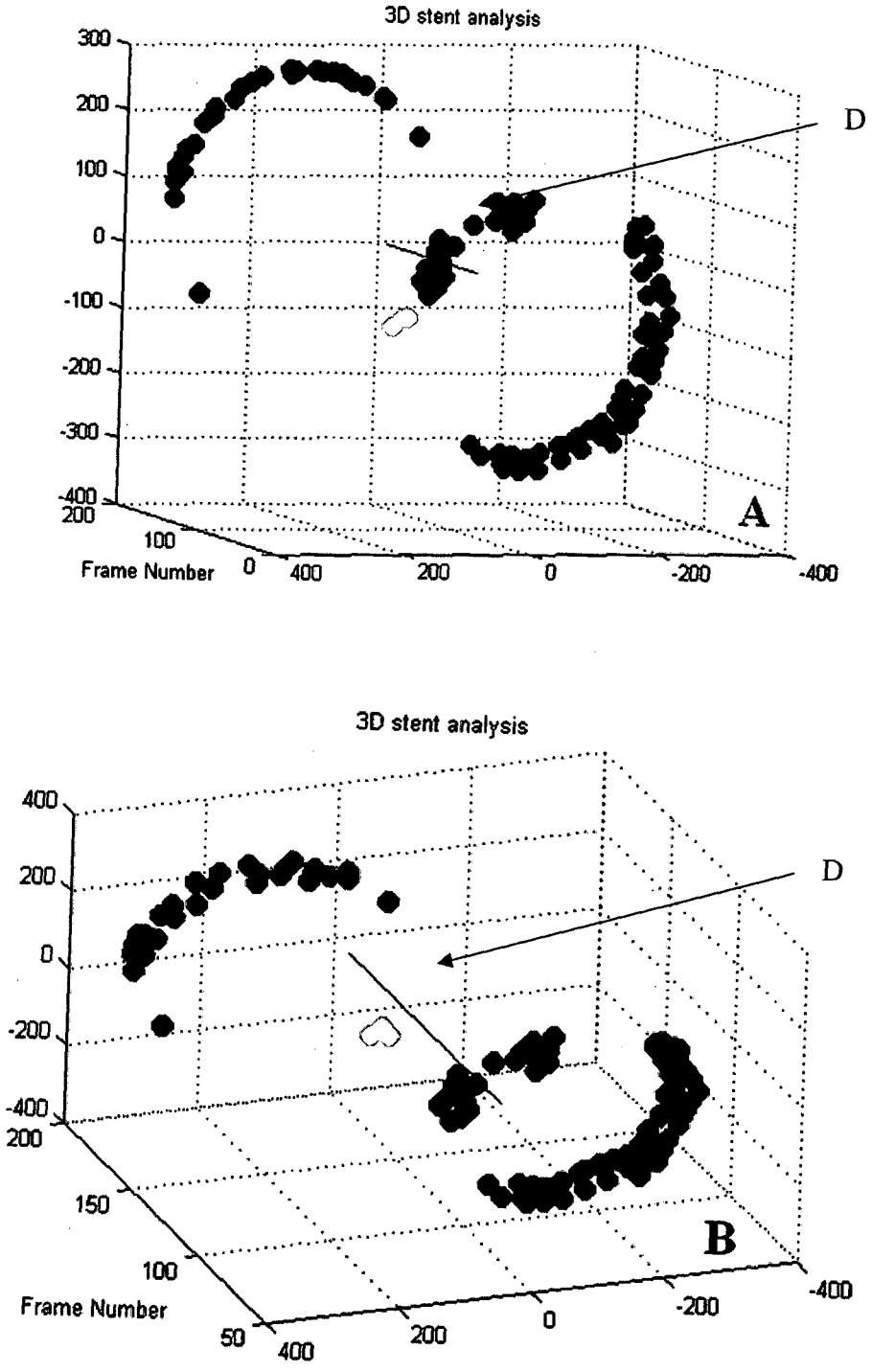
3D stent analysis
300
200
100
0
-100
-200
-300
-400
200
100
Frame Number
0
400
200
0
-200
-400
D
A
3D stent analysis
400
200
0
-200
-400
200
150
100
Frame Number
50
400
200
0
-200
-400
D
B

Figure 15

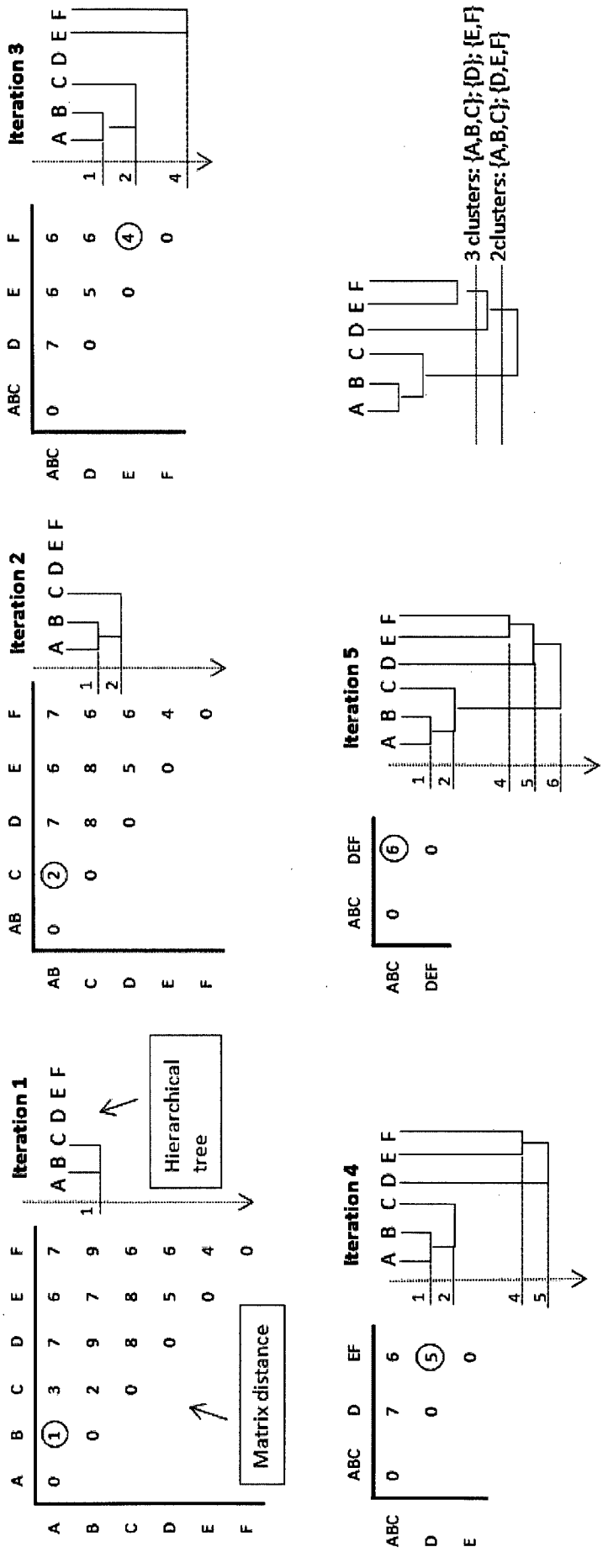
Iteration 1
Iteration 2
Iteration 3
Iteration 4
Iteration 5
Matrix distance
Hierarchical tree
3 clusters: {A,B,C}; {D}; {E,F}
2clusters: {A,B,C}; {D,E,F}

Figure 16

INTERNATIONAL SEARCH REPORT

International application No
PCT/BE2012/000017

A. CLASSIFICATION OF SUBJECT MATTER
INV. G06T7/00
ADD.

According to International Patent Classification (IPC) or to both national classification and IPC

B. FIELDS SEARCHED

Minimum documentation searched (classification system followed by classification symbols)
G06T

Documentation searched other than minimum documentation to the extent that such documents are included in the fields searched

Electronic data base consulted during the international search (name of data base and, where practicable, search terms used)
EPO-Internal, WPI Data, COMPENDEX, INSPEC

C. DOCUMENTS CONSIDERED TO BE RELEVANT

Category*	Citation of document, with indication, where appropriate, of the relevant passages	Relevant to claim No.
Y	US 2010/094127 A1 (XU CHENYANG [US]) 15 April 2010 (2010-04-15) abstract figures 1,9-19 paragraph [0051] - paragraph [0078] -----	1-32
Y	N. ROSENTHAL ET AL: "Unravelling the endovascular microenvironment by optical coherence tomography", EUROPEAN HEART JOURNAL, vol. 31, no. 2, 19 November 2009 (2009-11-19), pages 139-142, XP55034955, ISSN: 0195-668X, DOI: 10.1093/eurheartj/ehp481 page 139, right-hand column, last paragraph - page 140, left-hand column, paragraph first -----	1-32
	-/--	

[X] Further documents are listed in the continuation of Box C.

[X] See patent family annex.

* Special categories of cited documents :

"A" document defining the general state of the art which is not considered to be of particular relevance

"E" earlier application or patent but published on or after the international filing date

"L" document which may throw doubts on priority claim(s) or which is cited to establish the publication date of another citation or other special reason (as specified)

"O" document referring to an oral disclosure, use, exhibition or other means

"P" document published prior to the international filing date but later than the priority date claimed

"T" later document published after the international filing date or priority date and not in conflict with the application but cited to understand the principle or theory underlying the invention

"X" document of particular relevance; the claimed invention cannot be considered novel or cannot be considered to involve an inventive step when the document is taken alone

"Y" document of particular relevance; the claimed invention cannot be considered to involve an inventive step when the document is combined with one or more other such documents, such combination being obvious to a person skilled in the art

"&" document member of the same patent family

Date of the actual completion of the international search	Date of mailing of the international search report
10 August 2012	20/08/2012

Name and mailing address of the ISA/	Authorized officer
European Patent Office, P.B. 5818 Patentlaan 2 NL - 2280 HV Rijswijk Tel. (+31-70) 340-2040, Fax: (+31-70) 340-3016	Salvador, Elena

1

Form PCT/ISA/210 (second sheet) (April 2005)

C(Continuation). DOCUMENTS CONSIDERED TO BE RELEVANT

Category*	Citation of document, with indication, where appropriate, of the relevant passages	Relevant to claim No.
Y	BESL P J ET AL: "A METHOD FOR REGISTRATION OF 3-D SHAPES", IEEE TRANSACTIONS ON PATTERN ANALYSIS AND MACHINE INTELLIGENCE, IEEE SERVICE CENTER, LOS ALAMITOS, CA, US, vol. 14, no. 2, 1 February 1992 (1992-02-01), pages 239-256, XP000248481, ISSN: 0162-8828, DOI: 10.1109/34.121791 abstract Section IV Section V Section VI.A	1-32
Y	UGHI G J ET AL: "Automatic segmentation of in-vivo intra-coronary optical coherence tomography images to assess stent strut apposition and coverage", THE INTERNATIONAL JOURNAL OF CARDIAC IMAGING, KLUWER ACADEMIC PUBLISHERS, DO, vol. 28, no. 2, 24 February 2011 (2011-02-24), pages 229-241, XP035021771, ISSN: 1573-0743, DOI: 10.1007/S10554-011-9824-3 abstract Section "Methods" Section "Further Developments"	1-32
Y	SERHAN GURMERIC ET AL: "A New 3-D Automated Computational Method to Evaluate In-Stent Neointimal Hyperplasia in In-Vivo Intravascular Optical Coherence Tomography Pullbacks", 20 September 2009 (2009-09-20), MEDICAL IMAGE COMPUTING AND COMPUTER-ASSISTED INTERVENTION Â MICCAI 2009, SPRINGER BERLIN HEIDELBERG, BERLIN, HEIDELBERG, PAGE(S) 776 - 785, XP019130527, ISBN: 978-3-642-04270-6 abstract Sections 1, 2, 3 figures 5,6,7	1-32
A	GARRET T BONNEMA ET AL: "An automatic algorithm for detecting stent endothelialization fAn automatic algorithm for detecting stent endothelialization from volumetric OCT datasets", PHYSICS IN MEDICINE AND BIOLOGY, TAYLOR AND FRANCIS LTD. LONDON, GB, vol. 53, no. 12, 21 June 2008 (2008-06-21) , pages 3083-3098, XP020133865, ISSN: 0031-9155 the whole document	1-32

1

INTERNATIONAL SEARCH REPORT

Information on patent family members

International application No
PCT/BE2012/000017

Patent document cited in search report	Publication date	Patent family member(s)	Publication date
US 2010094127 A1	15-04-2010	AU 2009305771 A1	22-04-2010
		CA 2728662 A1	22-04-2010
		EP 2344020 A1	20-07-2011
		JP 2012505669 A	08-03-2012
		US 2010094127 A1	15-04-2010
		WO 2010045386 A1	22-04-2010